AD NUMBER

AD873241

NEW LIMITATION CHANGE

TO

Approved for public release, distribution unlimited

FROM

Distribution authorized to U.S. Gov't. agencies and their contractors; Administrative/Operational Use; Jun 1970. Other requests shall be referred to Commander, Air Weather Service [MAC], Attn: DN, Scott AFB, Il 62225

AUTHORITY

AFWA ltr, 19 Apr 2005

Technical Report 234

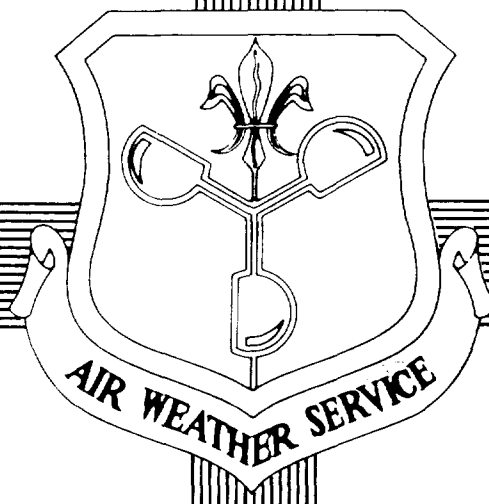

A MODEL of IONOSPHERIC TOTAL ELECTRON CONTENT

By

ALLAN C. RAMSAY

MAJOR USAF

HEADQUARTERS AIR WEATHER SERVICE

PUBLISHED BY

AIR WEATHER SERVICE (MAC)

UNITED STATES AIR FORCE

JUNE 1970

PREFACE

Ionospheric total electron content has a significant effect on time-delay measurements of transionospheric radio signals. Radio-ranging techniques used by radar and future satellite navigation systems must account for the variable time-delay introduced by the ionosphere.

This report presents a method for specifying or predicting the total electron content of the undisturbed mid-latitude ionosphere during the maximum phase of the solar cycle. This report is intended to benefit developers and operators of transionospheric range-measuring systems; it is operationally oriented, and is not intended as a review paper on global electron content or as a discourse on ionospheric physics.

I gratefully acknowledge the cooperation and assistance of both the Air Force Cambridge Research Laboratories (particularly J. A. Klobuchar, in the development and refinement of this electron-content model) and Major E. W. Friday, Jr., Hq Air Weather Service, who undertook the effort of preparing the Appendix to this report.

ALLAN C. RAMSAY, Major, USAF
Hq Air Weather Service
Scott AFB, Illinois 62225
May 1970

TABLE OF CONTENTS

LIST OF ILLUSTRATIONS

LIST OF TABLES

LIST OF SYMBOLS

B	-	Basic component of solar 10.7-cm radio flux.
C_o	-	Basic component of "standard" total electron content.
C	-	Constant of proportionality relating total electron content to the active-region component of solar radiation.
e	-	Electron charge (4.8×10^{-10} esu)/or electrons.
f	-	Frequency (Hz or mHz).
f_oF2	-	Critical frequency of F2 region.
F10	-	Daily value of solar 10.7-cm radio flux (10^{-22} watts/m^2/Hz).
$\overline{F10}_x$	-	Mean value of F10 over x days.
h	-	Height above earth's surface.
J	-	Factor relating TEC at any site to TEC at standard site (Section F: MOD III).
L	-	Factor relating TEC at any site to TEC at standard site (Section E: MOD II).
m	-	Electron mass (9.1×10^{-28} gm).
n	-	Refractive index.
N	-	Electron number density.
N_mF2	-	Maximum number density of electrons in F2 region.
r	-	Radius of earth.
R	-	Range error (meters).
TEC	-	Total Electron Content (10^{17} e/m^2).
θ	-	Zenith angle; angle between ray direction and the zenith at ionospheric penetration point.
τ	-	Slab thickness (km).
φ	-	Latitude.
χ	-	Noon solar zenith angle.
ω	-	Angular frequency (rad/sec).

Subscripts:

i	-	Referring to any point.
s	-	Referring to the standard point: ionospheric penetration between Hamilton, Massachusetts, and ATS-3; near 40°N 75°W.

p - Referring to peak value in diurnal curve.

sp - Referring to peak diurnal value at standard point.

x - Number of days over which $\overline{F}$ is meaned.

A MODEL OF IONOSPHERIC TOTAL ELECTRON CONTENT

SECTION A — INTRODUCTION

Organization

This report is written for application to a specific and limited operational problem: that of accounting for ionospheric time delay in VHF and UHF transionospheric range-measuring systems. It provides only the briefest background on the ionosphere; emphasis is given to the development and presentation of models of ionospheric total electron content. The models have been constructed primarily for operational utility rather than scientific elegance. Seasonal, diurnal, and solar-radiation-related variation in total electron content are modeled; impulsive changes related to geomagnetic disturbances are not modeled, but are described qualitatively.

The number of references used in this report has been minimized, and references have been restricted wherever possible to commonly-available sources. Readers should consult referenced material for in-depth discussions of physical processes and limitations of measuring techniques, and for more extensive bibliographies.

The report begins with a brief review of the source of range errors, a description of the earth's ionosphere, and a description of relevant portions of the solar radiation spectrum. Section D presents a basic means of specifying or predicting peak daily values of total electron content at a "standard" mid-latitude location. "Standard" refers to a site for which considerable data were available for specifying peak daily values of electron content and its diurnal variation. The "standard" for work presented here is the AFCRL Sagamore Hill Radio Observatory. Provision is made for the artificial construction of a typical diurnal curve of total electron content. Section E extends the "standard" electron-content peak value and the empirical diurnal variation of Section D to other locations through the use of ionospheric climatology. Section F again applies ionospheric climatology to the "standard" peak-value prediction generated in Section D, but additional assumptions are made to eliminate problems in timing of the diurnal variation. The version presented in Section F is the recommended general-purpose total-electron-content model. Section G describes areas of investigation that would be most likely to improve the validity and embraciveness of the model; slab thickness variations, solar cycle variations, and geomagnetic-disturbance effects are discussed.

Range Measurements

The determination of transmitter-to-target range by measuring the transit time of radio signals is a technique that will be used by Air Force radar and navigation systems for years to come. Range is determined simply and directly by multiplying the transit time of an electromagnetic signal by the velocity of signal propagation. However, where the refractive index of the propagating medium differs from unity, the velocity of the signal is decreased, and inferred ranges can be in error.

For radio signals propagating within the troposphere, range errors (differences between inferred and geometric ranges) are independent of the frequency of the signal and reach a maximum of about 100 meters [19]. For radio signals which travel through the ionosphere, however, range errors whose magnitude is inversely proportional to the square of the frequency can sometimes be measured in kilometers. The major range errors introduced in transionospheric VHF-UHF signals can be accounted for if the nature of the propagating medium is known.

Ionospheric Time Delay/Range Error

The index of refraction of the ionosphere can be defined by

$$(1) \qquad n = \left(1 - \frac{4\pi N e^2}{m \omega^2}\right)^{\frac{1}{2}}$$

when electron collision frequency and magnetic-field effects are ignored ([4], p. 390). Note that the refractive index is directly proportional to the electron density and inversely proportional to the square of the frequency of the propagating signal. This index of refraction causes the velocity of propagation to be less than that in free space, and, hence, introduces an excess time delay or range error. The range error, in meters, can be expressed by

$$(2) \qquad R = \frac{40.3}{f^2} \int_0^s N \, ds$$

where the frequency, f, is in Hz and the integrated electron content along the ray path is in electrons/m^2 [16]. Note that the range error is inversely proportional to the square of the frequency of the propagating signal and directly proportional to the total number of electrons along the ray path. Typical range errors for 100, 200, and 500 mHz signals are illustrated in Figure 1.

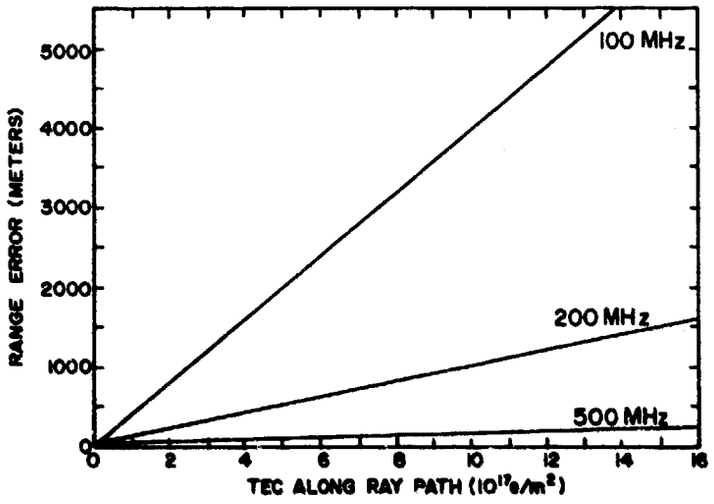

Figure 1. Range Error Versus Total Electron Content.

SECTION B — THE IONOSPHERE

Production/Loss Mechanisms

The earth's ionosphere is produced primarily by the ionization of neutral atmospheric constituents by solar radiation; ionizing radiation includes particles, ultraviolet, and x-ray. Because this report is concerned mainly with the upper regions of the ionosphere (the F2 layer and the "topside"), it is most concerned with the principal source of ionization in the F region: solar Extreme Ultraviolet (EUV) radiation from 200-800 Å.

Electrons are lost by recombination with positive ions or by attachment to neutral atoms.

The balance between production and loss processes in the F region is a complex function of variable radiation and a highly-variable chemistry of the atmospheric constituents (see Craig [4], Chapter 9; Kelso [14], Chapter 3).

Transport of ionization along magnetic field lines is also an important consideration in the F region. Advection of electrons into or out of an area of interest must be thought of as an additional gain/loss mechanism; this mechanism is thought to be responsible for many of the observed changes in electron content.

TEC Measurements

Figure 2 shows a typical vertical profile of daytime electron density in

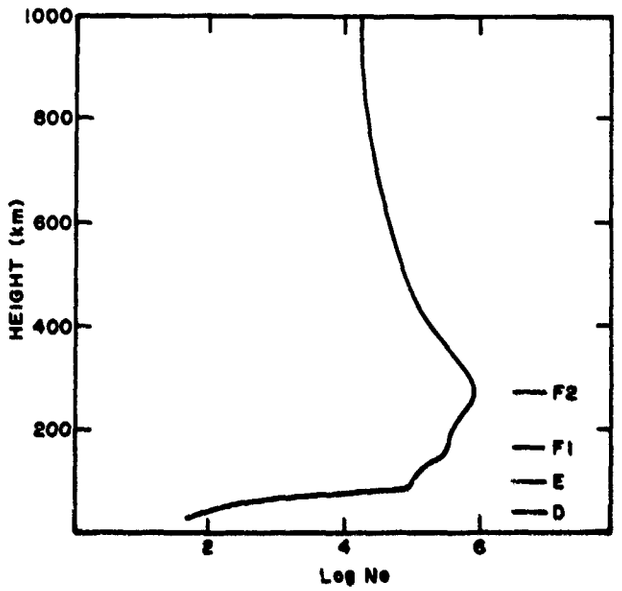

Figure 2. A Typical Daytime Ionospheric Profile, Electron Density Versus Height.

the ionosphere. The indicated D, E, and F layers in the lower ionosphere are of significance primarily to communicators who rely on the reflective characteristics of the ionosphere in the HF (3-30 mHz) region of the spectrum. The vertical profile must also be known by operators of range-measuring systems with a satellite terminal (or target) actually in the ionosphere. Systems to which this report relates are those using VHF-UHF signals which pass entirely through the ionosphere; for this reason, the entire integrated electron content in a one-meter-square vertical column from the surface to an altitude of a few thousand kilometers will be treated as a distinct parameter, analogous to a standard meteorological variable: surface pressure.

Note that standard ground-based measurements of ionospheric parameters are limited to that part of the ionosphere below the F2 peak in electron density. Roughly two-thirds of the electrons in the ionosphere are found above the F2 peak and hence are screened from conventional ground-based observations. An important relationship exists between the peak electron density, N_mF2, and the F2-region critical frequency, f_oF2 ([4], p. 291):

$$(3) \qquad N_mF2 = \left(\frac{\pi m}{e^2}\right) f^2 = 1.24 \times 10^{-8} \, (f_oF2)^2$$

There are a number of techniques that can be used to make direct observations of total electron content. The great majority of data available today have been obtained by analyzing the rotation of the place of polarization of VHF signals transmitted by satellite; this Faraday rotation technique is well documented [8] [23] and is accepted as an accurate and useful measure of TEC up to an altitude of a few thousand kilometers. Faraday rotation is proportional to the product of electron density and the magnetic field strength along the ray path. A great deal of literature is available on the major limitation to this technique: the need to include effects of the geomagnetic field weighted by the electron density profile [1] [26]. In addition to errors introduced by an assumption of magnetic field strength at the centroid

of the vertical profile along any penetrating ray, the method does not count electrons at higher altitudes where the strength of the earth's field is too low to contribute to the rotation effect. The data used in the development of this TEC model were obtained at the Air Force Cambridge Research Laboratories' Sagamore Hill (Mass.) Radio Observatory by the Faraday rotation technique, and the model is intended to specify and predict values of TEC as measured through Faraday rotation. The true total content between the earth and, say, a geostationary satellite, will be perhaps 10%-15% higher than the values given here.

Vertical Total Electron Content

The large-scale morphology of mid-latitude TEC is well illustrated in Figure 3 [16]. Marked seasonal and diurnal changes, as well as day-to-day fluctuations, are evident. (For a description of the complexities of worldwide TEC morphology, see Klobuchar [17].) TEC behavior is similar in many respects to f_0F2, the critical frequency of the F2 layer; this fact is fully exploited in the development of the TEC models in this report. The qualitative similarities are particularly noticeable in the seasonal and diurnal variations; the well-documented (but little understood) winter or seasonal anomaly in f_0F2 also shows up in the TEC observations. The winter anomaly is the phenomenon of higher Northern Hemisphere mid-latitude f_0F2s in December than in June (see Rishbeth and Garriott [21], Chapter V).

In following sections of this report, it will be convenient not to have to work with an ionosphere such as the one shown in Figure 2; an ionosphere having a single electron density, constant with height, is much easier to manipulate. An artificial ionosphere having a constant electron density chosen equal to maximum density in the real-world ionosphere, N_mF2, is shown in Figure 4. The thickness, τ, of such a rectangular ionosphere is chosen so that

$$\tau = \frac{TEC}{N} \tag{4}$$

where N is the single-valued electron density and TEC is the vertical total content of that same real-world ionosphere.

The parameter, τ, is called the slab thickness, and it plays a major role in TEC modeling for the following reason. Note that, if Equation (3) is substituted in Equation (4),

$$\tau = \frac{TEC}{1.24 \times 10^{-8} \, (f_0F2)^2}$$

or

$$TEC = 1.24 \times 10^{-8} \, (f_0F2)^2 \, \tau \tag{5}$$

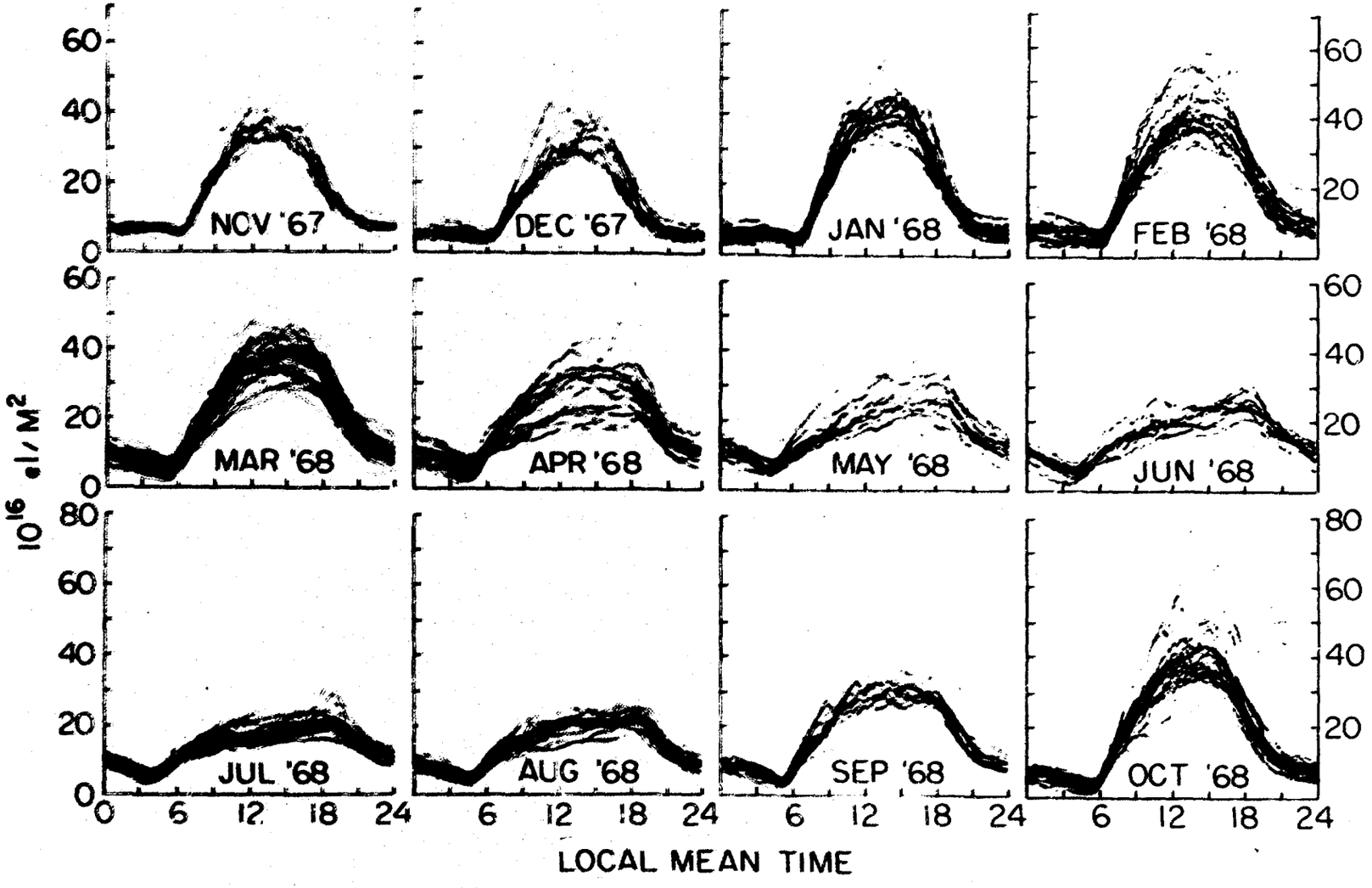

Figure 3. Total Equivalent Vertical Electron Content from Hamilton, Massachusetts (looking towards ATS-3).

TEC can thus be predicted (or specified) if one has information on the behavior of the F2 critical frequency and the slab thickness. The climatology of f_oF2 is well-known; numerical map functions for the worldwide variation of monthly median f_oF2 are prepared routinely by the Environmental Science Services Administration (ESSA), and both real-time observations and short-range forecasts of f_oF2 are available for USAF operational applications from the Air Weather Service Aerospace Environmental Support Center. The ESSA monthly median predictions [13] are used in the following TEC model as valid climatological descriptions of the lower F region (f_oF2).

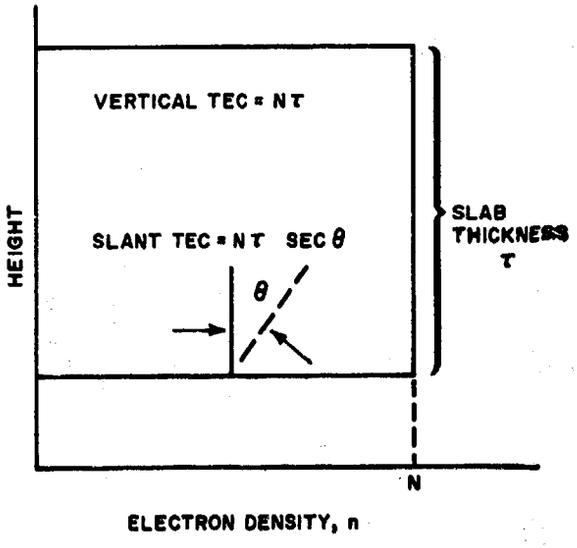

Figure 4. An Artificial Ionosphere: Electron Density Versus Height.

Slant Total Electron Content

Operational applications of TEC models will seldom involve vertical ray paths. Because vertical content is modeled and slant content must be applied operationally, a correction factor must be applied to modeled TEC values. Taking the rectangular ionosphere as an example (Figure 4), it can be seen that the slant TEC is related to the vertical TEC by

$$(TEC)_{slant} = (TEC)_{vertical} \text{ Sec } \theta$$

where θ is the angle between the ray direction and the zenith. In the real-world ionosphere a mean value of Sec θ, weighted by the electron density profile, must be determined. This weighted mean Sec θ is normally selected at an altitude of 350-400 km. The zenith angle of the ray at the ionospheric penetration point (at, say, 400 km) is a function of the elevation angle of the ray at the surface [5]:

$$\text{Sin } \theta = \frac{r}{r+h} \text{ Cos } \epsilon$$

or

$$\text{Sec } \theta = \left[1 - \left(\frac{6378}{6378 + 400}\right)^2 \text{Cos}^2 \epsilon\right]^{-\frac{1}{2}} \quad (6)$$

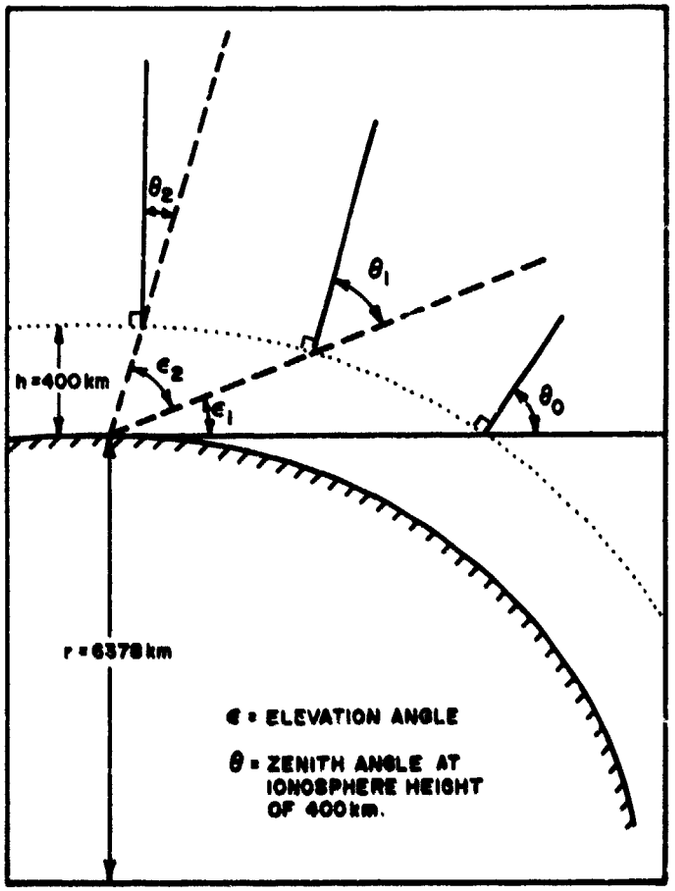

Figure 5. Geometry of Ionospheric Penetration.

Figure 5 illustrates the effect of elevation angle on penetration-point zenith angle; note the maximum θ at an elevation angle of 0°. θ decreases to 0° at an elevation angle of 90°.

Values of Sec θ for varying elevation angles can be determined from Figure 6. Note the maximum value of Sec θ = 2.95 for a 0° elevation angle. Thus, the slant TEC can be nearly three times greater than the vertical TEC at the ionospheric penetration point.

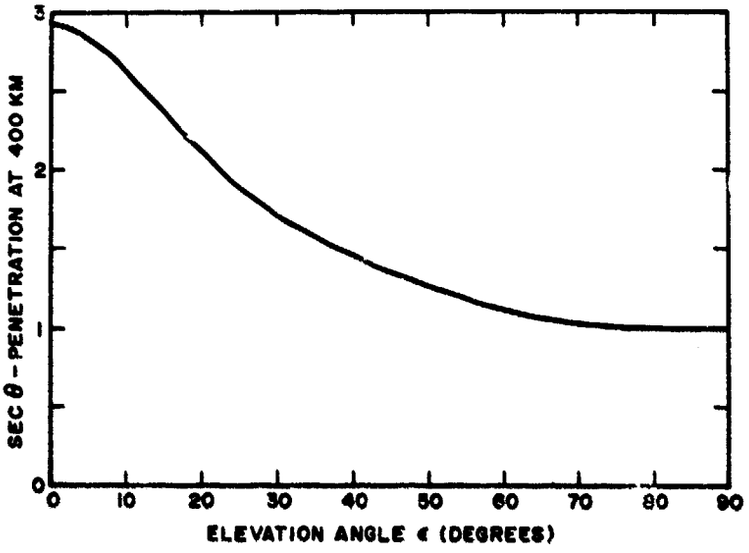

Figure 6. Sec θ Versus Elevation Angle.

SECTION C — SOLAR RADIATION

The EUV radiation that produces the upper ionosphere is emitted from the hot, tenuous gases in the lower solar corona. Direct observations of solar EUV can be made only from satellite platforms because the radiation is completely absorbed by the atmosphere before it can reach the earth's surface.

Solar radiation in radio wavelengths is emitted by the same region of the sun's atmosphere, and observations of solar radio noise have been used to infer changes in EUV radiation (COESA [3], Part 3). Solar radio noise at a wavelength of 10.7 cm has been observed continuously since the late 1940s; this measure of the sun's radio output (in watts/m^2/Hz) has been successfully used in models of neutral density at satellite altitudes as a measure of EUV heating of the upper atmosphere. The radio-flux parameter, F10 (units of 10^{-22} watts/m^2/Hz), is observed by the National Research Council of Canada, Ottawa, and by the Air Force Cambridge Research Laboratories, Sagamore Hill, Massachusetts. Data are readily available to operational and research agencies from the Air Weather Service Space Environmental Support System. F10 is used in this study to model solar EUV radiation. References to F10 should also be interpreted as references to solar EUV.

It is possible to consider the daily values of F10 as consisting of two components [22]: (1) a basic component, associated with a hypothetical sunspot-free sun, and (2) an active-region component (also known as the plage

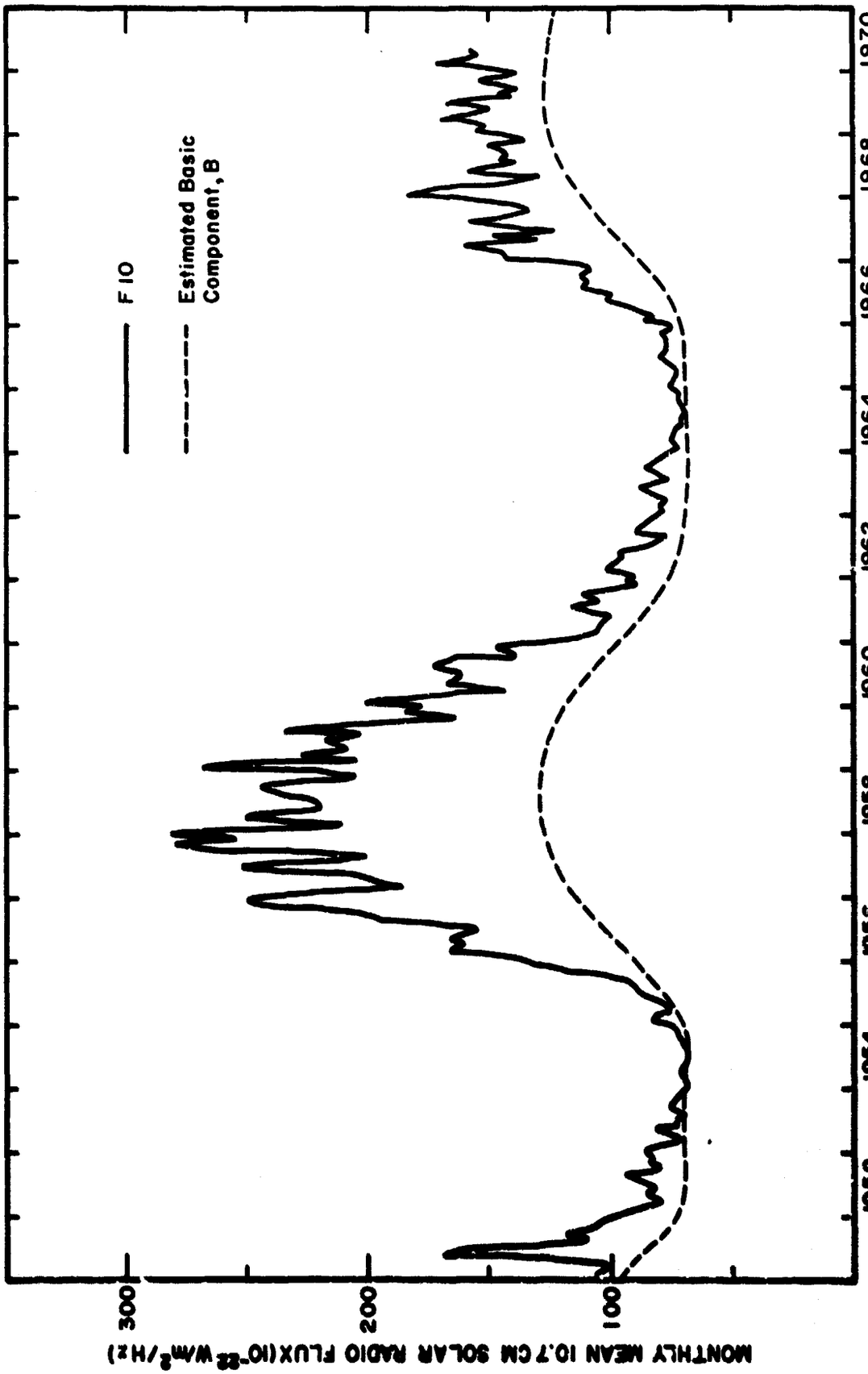

Figure 7. Solar Cycle Variation of 10.7-cm Solar Radio Flux, F10.

component or the slowly-varying component), associated with the higher coronal temperatures and densities above individual centers of activity on the sun's surface. The basic component varies with the 11-year solar cycle, and the active-region component shows both strong day-to-day variations and a 27-day periodicity corresponding to the rotation of active regions across the visible disk of the sun. Typical monthly mean values of F10 for the last 20 years are shown in Figure 7. A smoothed estimate [10] of the background component, B, obtained during Sunspot Cycle number 19 (1954-1964) is also shown in Figure 7. The background component varies from 68-70 units at solar minimum to an estimated 130 units at solar maximum. The value of B at solar maximum may, indeed, vary from sunspot cycle to sunspot cycle; however, for the purpose of this study it is assumed that the solar radio (EUV) flux may be described by two components: (1) a background value, B (nearly constant during solar maximum or minimum years), and (2) an active region contribution, F10 - B, which varies with the movement, growth, and decay of centers of activity. Thus:

$$FLUX = B + (F10 - B)$$

SECTION D — TEC MODEL I

Assumption

The basic premise of the TEC model is that peak daily TEC values at a "typical" Northern Hemisphere mid-latitude location can be related to a measure of the solar EUV radiation; TEC changes associated with geomagnetic disturbances are not considered. For this effort, it is assumed that the peak daily TEC value for a "standard" mid-latitude station can be specified by:

$$(7) \qquad TEC_p = C_o + C_1 (F10 - B)$$

TEC Components

The first term of Equation (7), C_o, represents the TEC contribution of the solar background radiation, B. This term includes the seasonal changes in TEC caused by primarily terrestrial rather than solar sources. C_o is illustrated in Figure 8. This particular curve was derived from observed TEC values during sunspot maximum; suggestions for similar functions applicable to other stages of the solar cycle are given in Section C.

The second term in Equation (7) represents the TEC contribution of solar active-region radiation. A number of researchers [2] [7] [12] have reported both linear and logarithmic relationships between TEC and either solar radio flux or smoothed sunspot number; all report seasonal variations in the

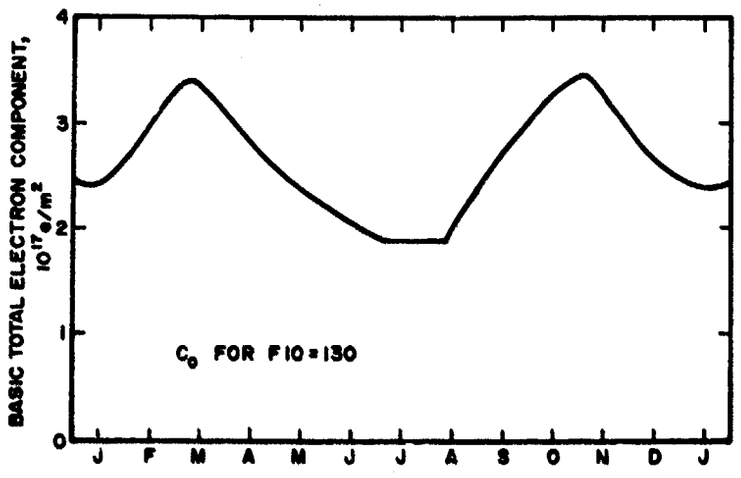

Figure 8. TEC Basic Component, C_o.

constants of proportionality. Because seasonal effects are modeled in the basic component of TEC, the relationship between TEC and solar active-region radiation is assumed to be constant throughout the year. (A test of TEC Model I, albeit on data from which the model was derived, showed no improvement in TEC specification when the value of C_1 was adjusted seasonally.) A representative value of the constant of proportionality, C_1, was selected from an analysis of the relationships reported in the literature; a value of 0.03 was chosen for use. A further refinement of the second term in Equation (7) is necessary to remove the "noisiness" of day-to-day fluctuations in F10; therefore, F10 is smoothed by the use of a mean value. For the specification of a monthly mean peak TEC value, the observed or predicted monthly mean F10 is used. For the specification or prediction of daily peak TEC values, a 5-day running mean of F10 ($\overline{F10}_5$) is used: $\overline{F10}_5$ computed for days D1 through D5 is used to specify the peak TEC values for D5 or to predict the peak value for D6. The daily peak TEC value is given by

$$TEC_p = C_o + 0.03\ (\overline{F10}_5 - B)$$

where, during sunspot maximum, C_o is determined from Figure 8 and B is 130 flux units, giving

$$(8) \qquad TEC_p = C_o + 0.03\ (\overline{F10}_5 - 130)$$

Diurnal Variation of TEC

A diurnal curve is constructed around the specified or predicted value of

TEC_p. The diurnal variation for the standard mid-latitude location is empirical in nature and is based on observations provided by AFCRL; the "standard" mid-latitude station is chosen to duplicate the AFCRL Sagamore Hill Radio Observatory, Massachusetts, with an ionospheric penetration point near 40°N 75°W. Five key values of TEC versus local time are selected and are merely connected with straight lines. The seasonal variation in the shape of the curve is produced by shifting the local time of the peak value. The construction of the curve is described below, and is illustrated in Figure 9.

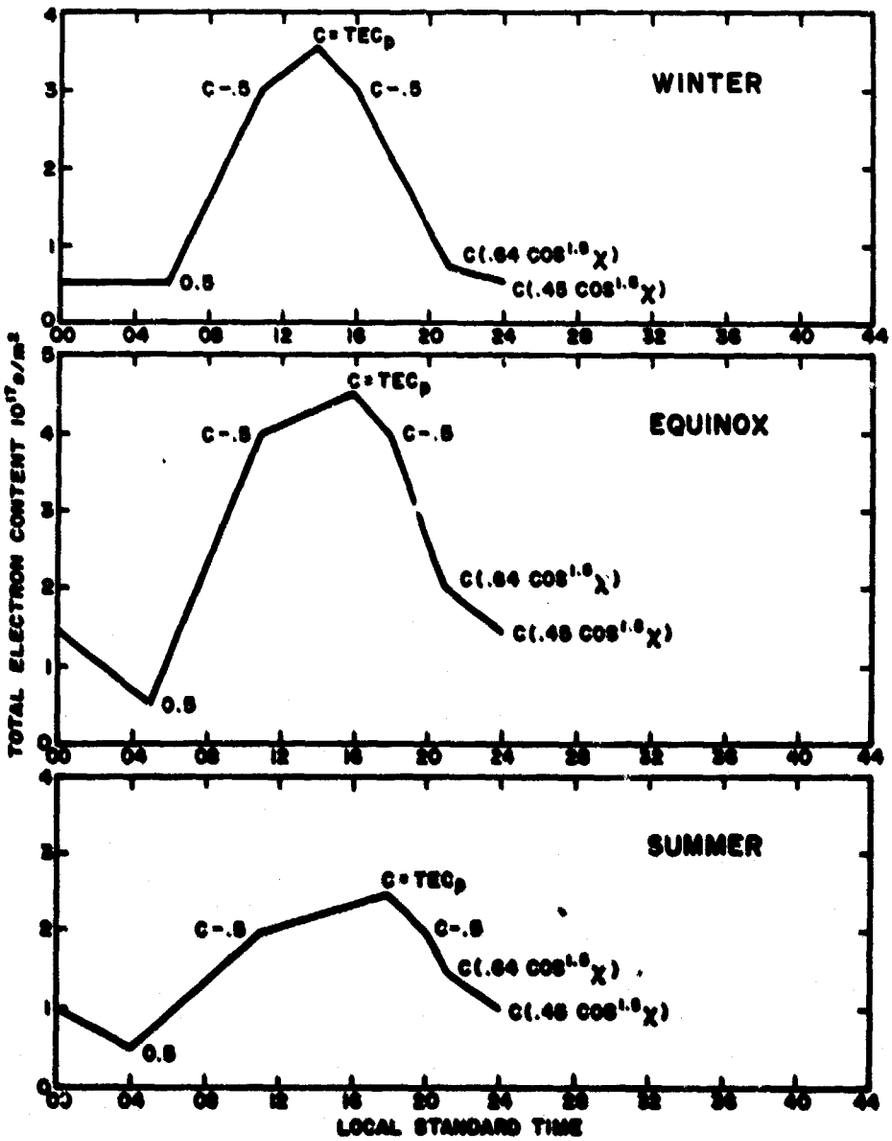

Figure 9. Seasonal Variation of Diurnal Curve Construction.

TEC MOD I

Predict diurnal TEC curve for standard mid-latitude site (40°N 75°W) for day D6:

a. Predict peak TEC, TEC_p:

(1) Determine basic component of TEC_p, C_o; use Figure 8.

(2) Determine 5-day running mean of F10, $\overline{F10}_5$, for days D1 through D5.

(3) Using Equation (8), $TEC_p = C_o + 0.03\ (\overline{F10}_5 - 130)$.

b. Specify local time of TEC_p:

Winter (Nov-Feb)	1400 LST
Equinox (Mar-Apr, Sep-Oct)	1600 LST
Summer (May-Aug)	1800 LST

c. Specify TEC = $TEC_p - 0.5 \times 10^{17}$ at 1100 LST and (Peak time + 2 hrs).

d. Specify TEC at 2100 and 2400 LST: See Figure 10 (Note: X is the peak solar zenith angle at 40°N on D6.)

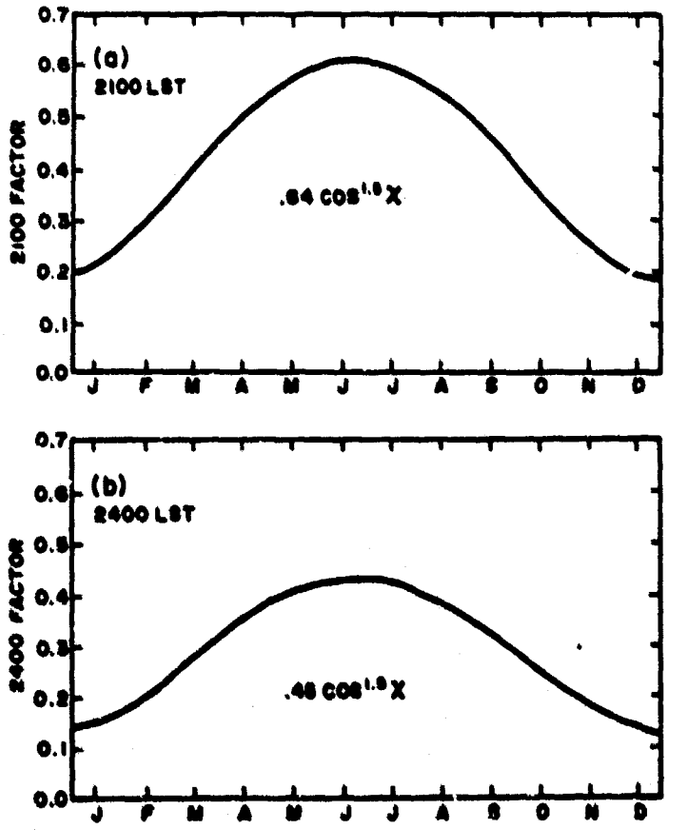

Figure 10. Factors for TEC Specification at 2100, 2400 LST.

(1) $TEC_{2100} = TEC_p\ (.64\ \cos^{1.5} \chi)$. Use Figure 10a.

(2) $TEC_{2400} = TEC_p\ (.45\ \cos^{1.5} \chi)$. Use Figure 10b.

e. Specify TEC at sunrise = 0.5×10^{17}

Winter 0600 LST
Equinox 0500 LST
Summer 0400 LST

Example of TEC MOD I

A specification of the monthly median diurnal curve for 40°N 75°W, April 1969, is illustrated below. Using the data in Table 1, the observed monthly mean of F10 is used in place of $\overline{F10}_5$ which would be used for daily TEC predictions.

Step 1. $C_o = 2.8 \times 10^{17}$

$\overline{F10}_{30} = 155$

$TEC_p = [2.8 + 0.03\ (25)] \times 10^{17}$

$= 3.6 \times 10^{17}$

Step 2. Time of TEC_p = 1600 LST

Step 3. TEC at 1100, 1800 LST = 3.1×10^{17}

Step 4. TEC at

2100 = 3.6×10^{17} (.50)

= 1.8×10^{17}

2400 = 3.6×10^{17} (.35)

= 1.4×10^{17}

Step 5. TEC at sunrise (0500 LST)

= 0.5×10^{17}

Step 6. Points are connected with straight lines; a comparison with observed data is shown in Figure 11.

TABLE 1

TEC MOD I DATA

DATE (1969)	F10	$\overline{F10}_5$	C_o	TEC_p
27 Mar	178	--	--	--
28	178	--	--	--
29	182	--	--	--
30	183	--	--	--
31	186	181	--	--
1 Apr	189	184	3.1	4.6
2	191	186	3.1	4.7
3	190	188	3.0	4.7
4	177	187	3.0	4.7
5	176	185	3.0	4.7
6	163	179	3.0	4.7
7	155	172	3.0	4.5
8	148	164	3.0	4.3
9	144	157	2.9	3.9
10	149	152	2.9	3.7
11	151	149	2.9	3.6
12	156	150	2.9	3.5
13	173	155	2.9	3.5
14	179	162	2.8	3.6
15	181	168	2.8	3.8
16	167	171	2.8	4.0
17	155	171	2.8	4.0
18	147	166	2.8	4.0
19	146	159	2.8	3.9
20	149	153	2.7	3.6
21	157	151	2.7	3.4
22	148	149	2.7	3.3
23	144	149	2.7	3.3
24	145	149	2.7	3.3
25	148	148	2.7	3.3
26	144	146	2.6	3.1
27	135	143	2.6	3.1
28	135	141	2.6	3.0
29	128	138	2.6	2.9
30	129	--	2.6	2.8

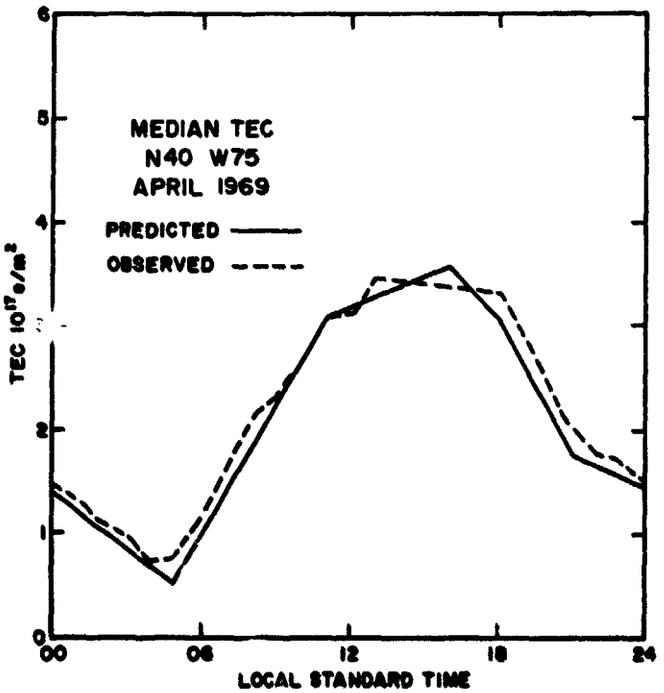

Figure 11. Specified and Observed TEC, April 1969.

SECTION E — TEC MODEL II

Assumption

TEC MOD II is designed to generate a diurnal curve for locations other than the "standard" mid-latitude station. The assumption necessary to convert the standard curve, $TEC_s(t)$, to any other location, $TEC_i(t)$, is that the slab thickness at any given local time is the same the world over: $\tau_i = \tau_s$. The few available comparisons of slab thickness at different stations [15] [24] indicate that the assumption is reasonable over middle latitudes. The assumption is not valid at equatorial latitudes, particularly during sunlit hours.

Derivation

Applying the assumption of identical diurnal slab-thickness variations at all points,

$$\tau_i(t) = \tau_s(t).$$

By Equation (4), then, at any given local time,

$$\frac{TEC_i}{N_i} = \frac{TEC_s}{N_s}$$

or

$$(9) \qquad TEC_i = TEC_s \frac{N_i}{N_s}$$

Substituting for N from Equation (3)

$$TEC_i = TEC_s \frac{(f_oF2_i)^2}{(f_oF2_s)^2}$$

or

$$(10) \qquad TEC_i = TEC_s \bullet L$$

where

$$(11) \qquad L = \left(\frac{f_oF2_i}{f_oF2_s}\right)^2$$

Application

The conversion factor, L, can be computed from an analysis of median f_oF2 predictions. One can then specify TEC at any point at a given local time by applying the L-factor to the standard TEC prediction at that local time. Table 2 shows an example of L-factors computed for longitudes 15°E-165°E for the month of April 1969; each L-factor is valid at 1100 LST at the different longitudes.

TABLE 2

L-Factors for 1100 LST, April 1969.

	East Longitude											
North Latitude	15	30	45	60	75	90	105	120	135	150	165	Mean
70	0.7	0.7	0.8	0.9	0.9	0.8	0.8	0.7	0.6	0.6	0.5	0.7
60	0.8	0.9	1.0	1.2	1.2	1.2	1.1	1.0	0.9	0.8	0.8	1.0
50	1.1	1.1	1.2	1.4	1.5	1.5	1.5	1.4	1.3	1.2	1.2	1.3
40	1.5	1.5	1.6	1.7	1.8	1.9	1.9	1.8	1.8	1.8	1.7	1.7
30	1.9	2.2	2.2	2.3	2.3	2.3	2.3	2.4	2.3	2.4	2.2	2.3
20	2.3	2.3	2.5	2.8	2.6	2.4	2.5	2.7	2.5	2.4	2.3	2.5

The TEC at 1100 LST at each point in the table would be computed by multiplying the standard TEC from Figure 10 at 1100 LST (3.1×10^{17} e/m^2) by the appropriate L-factor, as

$$TEC_{i,\ 1100\ LST} = TEC_{s,\ 1100\ LST} \cdot L_{i,\ 1100\ LST}$$

It is sometimes convenient to require L to be of the form

$$L = A \exp(-b\varphi)$$

where φ is geographic latitude. As an example of this form of L, the latitudinal variation of L at a given local time and given longitude (or range of longitudes) is plotted and a best-fit exponential for the 40°N-60°N region is determined. Figure 12 shows the mean Eastern Hemisphere L-factor versus latitude from Table 2; the best-fit exponential

$$L = 5.1 \exp(-.027\ \varphi)$$

is also shown. The illustrated curve is an exceptionally good fit, and is not expected in all cases, particularly at low latitudes.

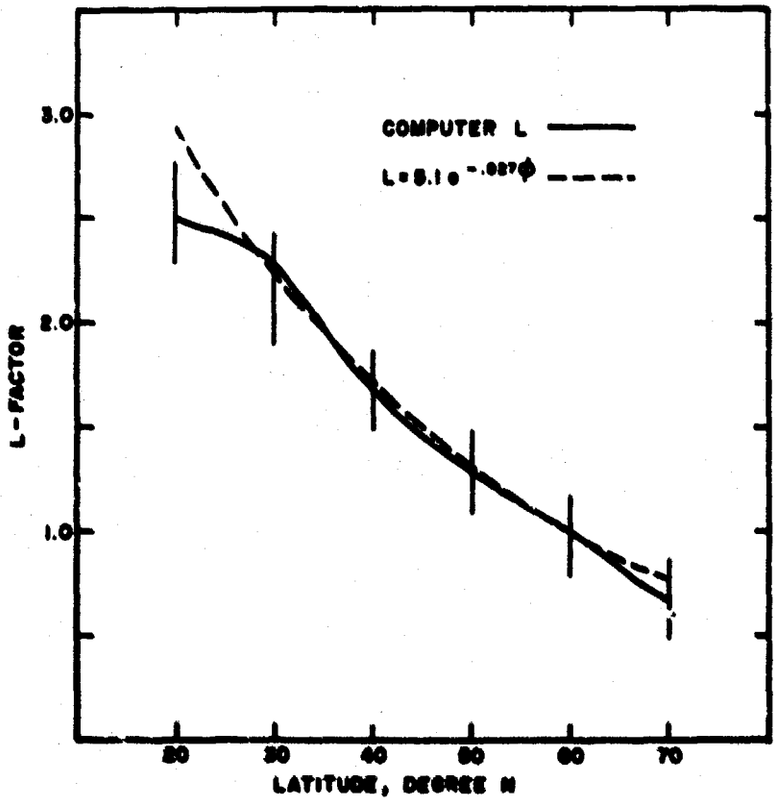

Figure 12. L-Factor Versus Latitude, 1100 LST.

Example of TEC MOD II

The specified monthly median TEC diurnal variation for Hawaii is derived for March 1967.

Step 1. The diurnal curve for the standard station is generated as in MOD I, using $\overline{F10}_{30} = 161$. The standard diurnal curve is shown in Figure 13c.

Step 2. Diurnal f_oF2 curves for both Hawaii and the standard station are shown in Figure 13a.

Step 3. The conversion factor, L, determined by the square of the ratio of the f_oF2 curves, is shown in Figure 13b.

$$L = \left(\frac{f_oF2_1}{f_oF2_s}\right)^2$$

Step 4. $TEC = TEC_s \cdot L$

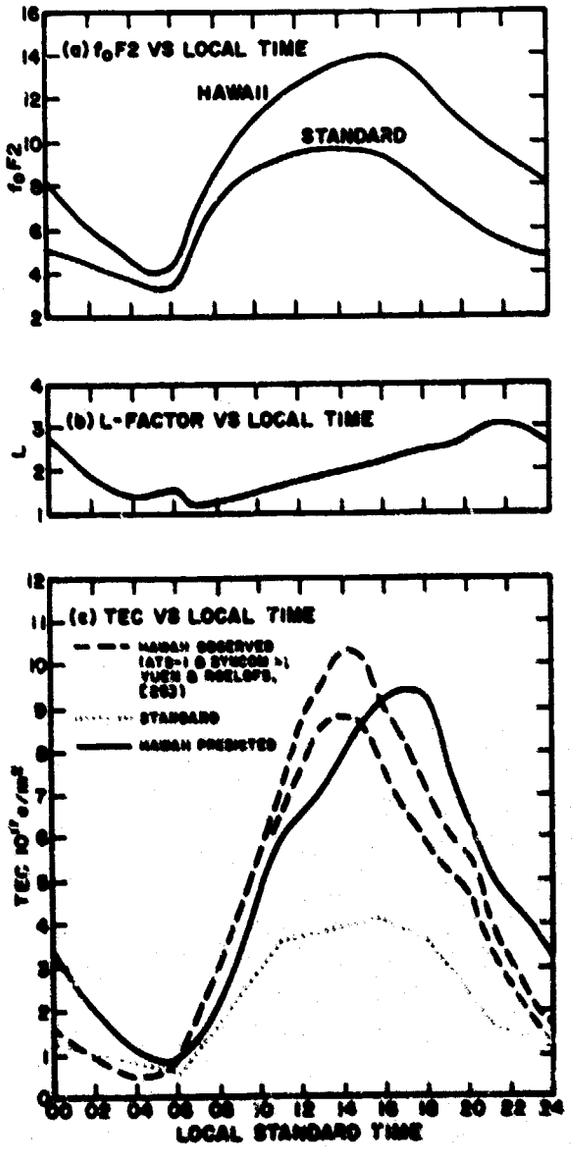

Figure 13. Example of TEC MOD II.

The modeled curve, defined by the product of the standard TEC curve in Figure 13a and the L-curve in Figure 13b, is shown in Figure 13c.

SECTION F — TEC MODEL III

Assumption

A prime deficiency of MOD II is the artificial control of the worldwide diurnal curves by the empirical constraints placed on the standard diurnal curve. A more general form of diurnal variation is obtained by allowing each location's TEC to vary as the local $(f_oF2)^2$. MOD II assumed equivalent slab thicknesses at all points at the same local time; an unspecified diurnal variation in τ was allowed. MOD III must assume an absolutely constant slab thickness. Because τ is known to have a considerable diurnal variation, this assumption introduces rather obvious errors. Slab thickness is chosen to be the standard-station slab thickness at the time of peak TEC, τ_{sp}.

Derivation

In this case, the peak TEC at location, i, is predicted similarly to MOD II, but without the artificial specification of the time of peak TEC. Each station's diurnal TEC curve is normalized to its $(f_oF2)^2$ diurnal peak value. Assume $\tau_i = \tau_{sp}$ = CONSTANT.

From Equation (4),

$$\frac{TEC_i}{N_i} = \frac{TEC_{sp}}{N_{sp}}$$

$$TEC_i = TEC_{sp}\,\frac{N_i}{N_{sp}}$$

$$TEC_i = TEC_{sp}\left(\frac{f_oF2_i}{f_oF2_{sp}}\right)^2 \tag{12}$$

or

$$TEC_i = TEC_{sp} \cdot J \tag{13}$$

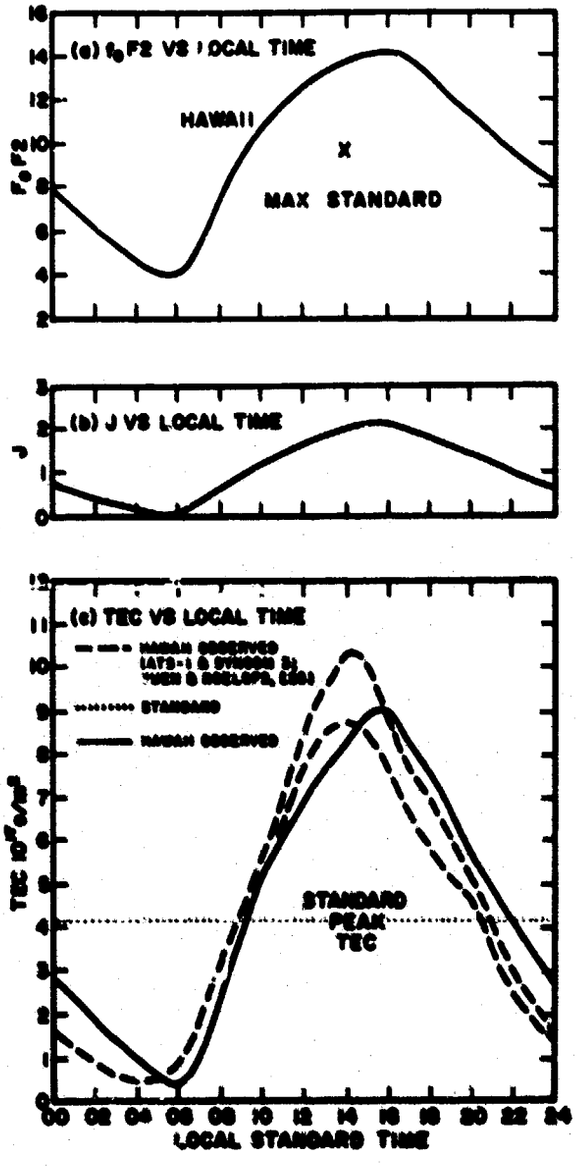

Figure 14. Example of TEC MOD III.

Application

To predict diurnal TEC curve for any location, i, for day D6:

a. Predict standard peak TEC, TEC_{sp}:

(1) Determine basic component of TEC_{sp}, C_o; use Figure 8.

(2) Determine 5-day running mean of F10, $\overline{F10}_5$, for days D1 through D5.

(3) $TEC_{sp} = C_o + 0.03\ (\overline{F10}_5 - 130)$.

b. Determine factor, J, relating TEC_{sp} to TEC_i:

(1) Determine peak value of f_oF2 diurnal variation at standard location: 40°N 75°W.

(2) Determine diurnal variation of f_oF2 at location, i.

(3) $$J(t) = \left(\frac{f_oF2_i(t)}{f_oF2_{sp}}\right)^2$$

c. $TEC_i(t) = TEC_{sp} \cdot J(t)$

TEC MOD III gives a reasonable estimate of mid-latitude diurnal TEC variations under geomagnetically quiet conditions. Derivations from absolute (measured) values are large at low latitudes at all times of day, and are largest at mid-latitudes during the night and post sunrise hours. The shapes of the diurnal curves are, however, more realistic at all latitudes than those in MOD II. While TEC absolute value errors are greater in MOD III, longitudinal TEC gradients inferred from the diurnal curve are more accurate. Improvements in this model must await additional knowledge of the worldwide morphology of slab thickness. The Appendix contains a general-purpose computer program for TEC MOD III predictions based on ESSA/ITS ionospheric predictions.

Example of TEC MOD III

The specified monthly median TEC diurnal variation for Hawaii is again derived for March 1967.

Step 1. The standard peak TEC value is determined as in MOD I.

$$TEC_{sp} = C_o + 0.03\ (\overline{F10}_{30} - 130) = 3.2 + 0.03\ (31) = 4.1 \times 10^{17}\ e/m^2$$

Step 2. Determine factor J:

$$J = \left(\frac{f_oF2_i}{f_oF2_{sp}}\right)^2$$

The predicted monthly median f_oF2 curve for Hawaii and the maximum f_oF2 for the standard location are shown in Figure 14a. J is shown in Figure 14b.

Step 3. $TEC_i = TEC_{sp} \cdot J$

The product of J (Figure 14b) and the standard peak TEC is shown in Figure 14c.

SECTION G — MODIFICATIONS

Geomagnetic Disturbances

The behavior of mid-latitude TEC during geomagnetic disturbances has so far resisted all attempts at modeling. A few general rules have been extracted from TEC observations [11] [20]:

a. TEC increases above normal quiet-day values during the first day of a sudden-commencement (SC) disturbance; the increase is typically greatest during pre-sunset hours on the first day of the disturbance. Disturbed values of TEC may be double the typical quiet-day values.

b. TEC is generally below quiet-day values for the remainder of the disturbance; the largest negative percentage deviations are observed between 0300-0600 LST. Mendillo, in a detailed study of 22 geomagnetic disturbances, reports apparent seasonal as well as storm-time characteristic TEC behavior.

c. There are no consistent relationships observed between standard geomagnetic indices (A_p, K) and TEC variations; TEC is apparently better related to storm phase.

d. There are indications that f_oF2 changes precede TEC changes by a few hours.

Slab Thickness

It is clear that one need go no further than Equation (5) to model TEC if the slab thickness is a known quantity. Klobuchar [18] is developing an expression for mid-latitude daytime τ (at Sagamore Hill, Massachusetts) of the form

$$(14) \qquad \tau = A + B \sin \frac{\pi}{12} (h - C) + E \sin \frac{\pi}{183} (d - F)$$

where A, B, C, E, and F are constants, h is the local time, and d is day of year. If this expression can be extended to other latitudes (and longitudes), then real-time observations (or short-range predictions) of f_oF2 could be used to specify (or predict) TEC with an expectation of high accuracy.

Until further definition of Equation (14) can be attained, it may be possible to improve the applicability of TEC MOD II or MOD III to low latitudes by modifying the assumption of a constant slab-thickness. Observations of monthly-median slab thickness at Sagamore Hill suggest a relationship between midday τ and the noon-time solar zenith angle of the form

$$\tau = A + B \cos^2 \chi$$

The $\cos^2 \chi$ relationship looks particularly good during the summer months and is illustrated in Figure 15. (See Goodman [9] for a presentation of a similar relationship between τ and $\cos \chi$ which is extended to an expression for TEC as a function of $\cos \chi$.) We may assume that similar relationships exist between slab thickness and χ at other latitudes; relationships may then be developed among slab thicknesses at different locations using $\cos \chi$ or $\cos^2 \chi$. Such relationships could then be applied to Equation (14) to specify τ at any point.

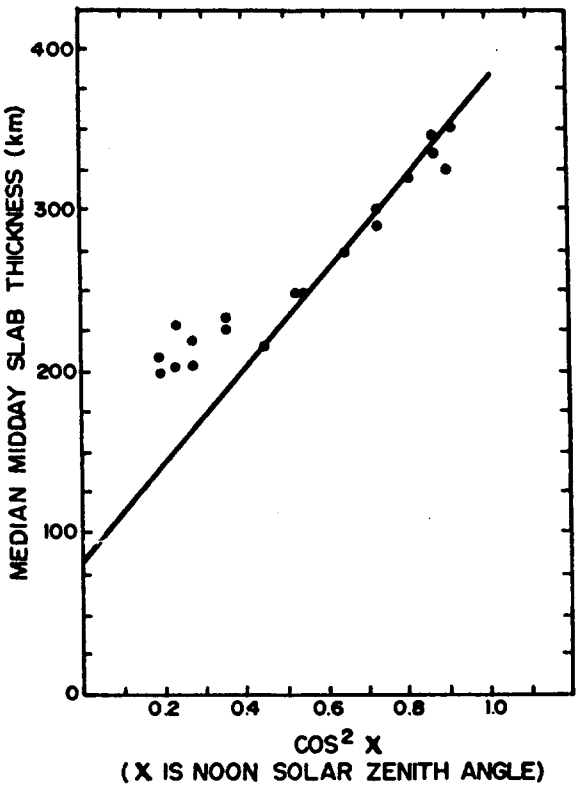

Figure 15. Midday Slab Thickness Versus the Square of the Cosine of the Noon Solar Zenith Angle.

Solar Cycle Variation of C_o

The term, C_o, in Equation (7) describes that component of TEC_p related to the meteorology of the earth's upper atmosphere and to the background component of solar ultraviolet radiation. C_o should, then, vary with the solar cycle. By combining data reported by Youakim and Rao [24] with Sagamore Hill observations, a relationship between the minimum annual (summer) C_o and solar background radiation, B, is estimated to be

$$(15) \quad \text{MIN } C_o = 0.13B$$

The amplitude of the semiannual C_o variation is estimated to be

$$(16) \quad \text{MAX } C_o - \text{MIN } C_o = 0.115B$$

Using Equations (15) and (16), it is possible to estimate the variation in C_o over the solar cycle. Suggested C_o curves for different phases of the solar cycle are presented in Figure 16. The shape of these curves may also vary with solar cycle. One particular aspect of the suggested C_o variation should be watched closely by operational agencies: the change from characteristic equinoctial to summer behavior is often observed to occur over a short-time span (say, on the order of weeks). The gradual seasonal changes in C_o indicated in Figures 8 and 16 may have to be adjusted to reflect a more rapid changeover from one season to another.

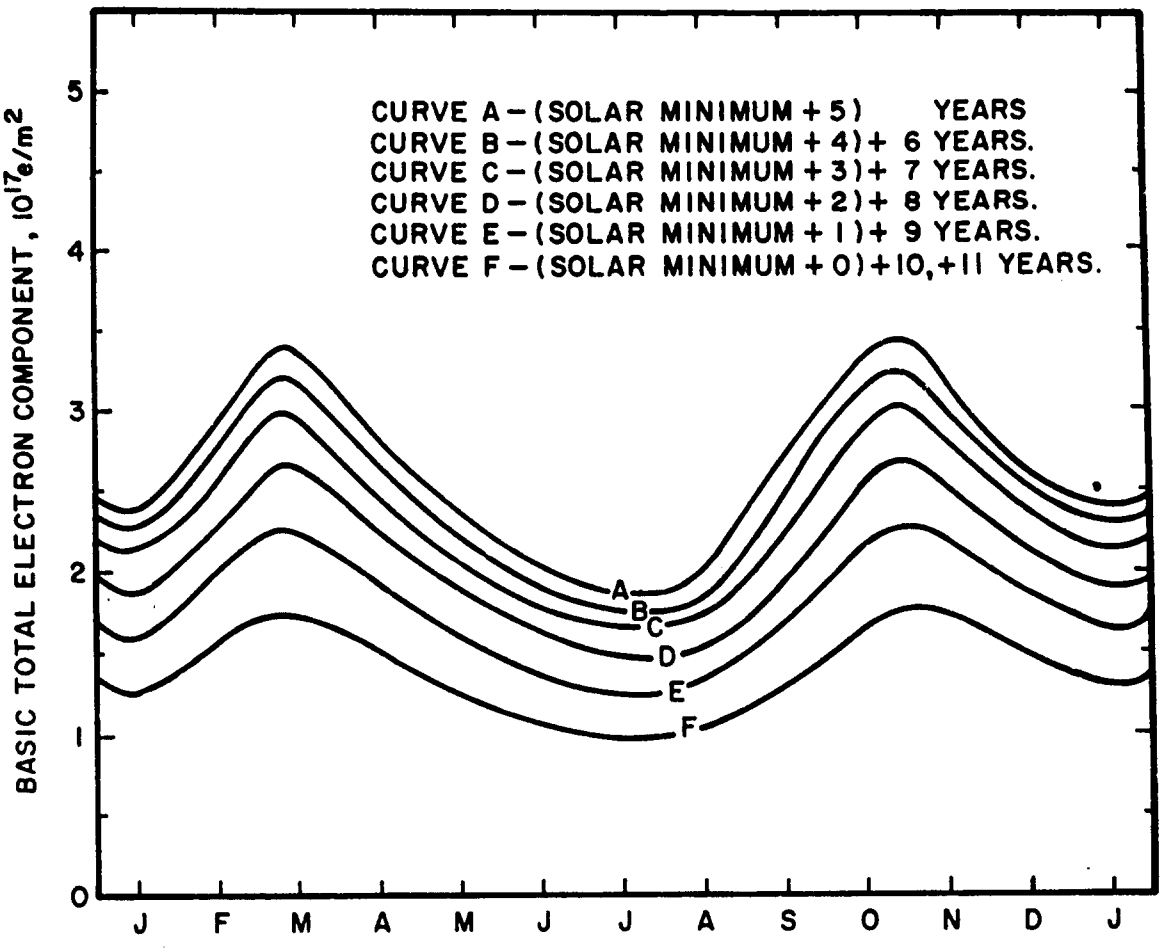

Figure 16. Solar Cycle Variation of C_o.

SECTION H — CONCLUSIONS

The TEC models presented in this report were generated in recognition of an immediate need for operationally-oriented data. The use of the models requires a minimum of resources: all are suitable for hand calculations, and requisite input data are readily available. Key points are reiterated:

a. Assumptions made in the derivation of the models have introduced significant limitations.

b. The models attempt to duplicate Faraday-rotation data, and hence account for approximately 90% of the true TEC between the earth and a geostationary satellite.

c. The models are applicable to an undisturbed Northern Hemisphere

mid-latitude ionosphere near the maximum of the solar cycle. They are not valid near the equatorial anomaly, in the auroral zone, or during geomagnetic disturbances.

The accuracies that may be expected are as follows:

a. Standard station monthly-median peak values should be accurate to within about 5%;

b. Standard station daily peak values should be accurate to within about 15%;

c. Specification/prediction of peak daily values at an arbitrary location should be accurate to within about 25%.

This report is concluded with an opinion: that it has underscored the need for far more investigation than has been accomplished to date. An operationally meaningful specification of a significant environmental parameter, such as TEC, must be valid everywhere the Air Force has to function — and this certainly includes auroral-zone and equatorial latitudes. It appears that the future of operational TEC specification lies in relating observable ionospheric parameters, such as f_oF2, to functions such as suggested by Klobuchar [Equation (14)] that could be applied anywhere in the world. All of which serves to emphasize the need for expanded research efforts.

REFERENCES

[1] Almeida, O. G., Garriott, O. K., and da Rosa, A. V.: "Determination of the Columnar Electron Content and the Layer Shape Factor of the Plasmasphere Up to the Plasmapause," Planet. Space Sci., Vol. 18, No. 2, February 1970, pp. 159-170.

[2] Bhonsle, R. V., da Rosa, A. V., and Garriott, O. K.: "Measurements of the Total Electron Content and the Equivalent Slab Thickness of the Mid-latitude Ionosphere," Radio Science, Vol. 69D, July 1965, pp. 929-937.

[3] Committee on Extension of the Standard Atmosphere (COESA), U.S. Standard Atmosphere Supplements, 1966, ESSA/NASA/USAF, US Government Printing Office, 1966, 289 p.

[4] Craig, R. A., The Upper Atmosphere: Meteorology and Physics, International Geophysics Series, Vol. 8, Academic Press, New York, 1965, 509 p.

[5] da Rosa, A. V.: "Propagation Errors in VHF Satellite to Aircraft Ranging," Stanford Radio Science Lab., NASA Contract NAS5-10102, Quarterly Report No. 4, January 1969.

[6] Davies, K.: Ionospheric Radio Propagation, National Bureau of Standards Monograph 80, US Government Printing Office, 1965.

[7] Galdon E. and Alberca, L. F.: "Influences of the Solar Activity on the Total Electron Content of the Ionosphere over Tortosa (1964-1968)," Scientific Report No. 3 (AFCRL-69-04). Contract AF 61(052)-924, 30 March 1969, 28 p.

[8] Garriott, O. K., Smith, F. L. III, and Yuen, P. C.: "Observations of Ionospheric Electron Content Using a Geostationary Satellite," Planet. Space Sci., Vol. 13, 1965, p. 829.

[9] Goodman, J. M.: "A Note on the Seasonal Variation of the Ionospheric Electron Content and Slab Thickness Over Washington, D. C.," Planet. Space Sci., Vol. 16, No. 8, August 1968, pp. 1073-1078.

[10] Hachenberg, O.: "Radio Frequency Emissions of the Sun in the Centimeter Wavelength Range: The Slowly Varying Sunspot Component," in: Solar System Radio Astronomy, J. Aarons, ed. Plenum Press, New York, 1965, pp. 95-108.

[11] Hibberd, F. H. and Ross, W. J.: "Variations in Total Electron Content and Other Ionospheric Parameters Associated with Magnetic Storms," J. Geophys. Res., Vol. 72, No. 21, November 1967, pp. 5331-5337.

[12] Houminer, Z.: "On the Variation of Ionospheric Electron Content with the Sunspot Cycle," in: Ionospheric Research Using Satellites, Annual Scientific Report No. 3, Radio Observatory, Haifa, Israel, February 1968.

[13] Jones, W. B., Graham, R. P., and Leftin, M.: Advances in Ionospheric Mapping by Numerical Methods, ESSA Technical Report ERL 107-ITS 75, Boulder, Colorado, May 1969, 76 p.

[14] Kelso, J. M.: Radio Ray Propagation in the Ionosphere, McGraw-Hill Book Co., Inc., New York, 1964, 408 p.

[15] Klobuchar, J. A. and Aarons, J.: "Electron Content Latitude Dependence March 1966 Period," Annales de Geophys., Vol. 24, No. 3, July-September 1968, pp. 885-888.

[16] Klobuchar, J. A.: "Propagation Delays of VHF Waves," in: A Survey of Scintillation Data and its Relationship to Satellite Communications, Agardograph Report 571, NATO, August 1969, pp. 89-92.

[17] Klobuchar, J. A.: "World Wide Morphology of Total Electron Content," Presented at AGARD Lecture Series No. 41, Introduction to VHF Satellite Navigation and Communication Systems, Eindhoven, Netherlands, and Ottawa, Canada, June 1970.

[18] Klobuchar, J. A.: Private communication, May 1970.

[19] Moreland, W. B.: "Estimating Meteorological Effects on Radar Propagation," Air Weather Service Technical Report 183, January 1965.

[20] Mendillo, M., Papagiannis, M. D., and Klobuchar, J. A.: "Mid-Latitude Ionospheric Variations During Magnetic Storms," in: Symposium on the Application of Atmospheric Studies to Satellite Transmissions, Ionospheric Physics Laboratory, Air Force Cambridge Research Laboratories, September 1969.

[21] Rishbeth, H. and Garriott, O. K.: Introduction to Ionospheric Physics, Academic Press, New York, 1969.

[22] Tanaka, H.: "Eleven-Year Variation of the Spectrum of Solar Radio Emission on the Microwave Region," Proc. Res. Inst. Atmospherics, Vol. 11, No. 41 (1964).

[23] Titheridge, J. E.: "Continuous Records of the Total Electron Content of the Ionosphere," J. Atmos. Terrest. Phys., Vol. 28, No. 12, December 1966, pp. 1135-1150.

[24] Youakim, M. Y. and Rao, N. N.: "Study of Ionospheric Electron Content from Observations at Different Stations," Technical Report No. 34, Ionosphere Radio Laboratory, University of Illinois, July 1968.

[25] Yuen, P. C. and Roelofs, T. H.: Atlas of Total Electron Content Plots, Vol. 3, University of Hawaii, 1967.

[26] Yuen, P. C., Roelofs, T. H., and Young, D. M. L.: "Corrections to Electron Content Data for Changes in Layer Height," J. Geophys. Res., Vol. 74, No. 1, January 1969, pp. 384-387.

APPENDIX

The computer subroutines listed in this appendix are designed to calculate the value of L in Equations (10) and (11) or J in Equations (12) and (13) for use in the calculation of total electron content. This program relies heavily upon the work described in ESSA Technical Report ERL107-ITS 75, May 1969, Advances in Ionospheric Mapping by Numerical Methods. Subroutines GK, SICOJT, DKSICO, DKGK are extracted directly from the report; the only changes made were those necessary to convert them to conventional FORTRAN IV. The subroutines TEC and SAGMAX will be described below.

Subroutine TEC will compute the value for any point at any time. The subscript i refers to the particular point desired; the subscript SAG refers to the reference value at Sagamore Hill Observatory. The subroutine calling sequences is (K, U, ALAT, ALON, AMAGLT, TIME, RATIO). The parameters are defined as follows:

K, U	Parameters contained in ESSA $f_o(F2)$ coefficients. This coefficient deck may be read with the READU subroutine described in ERL107-ITS 75.
ALAT, ALON	Latitude and longitude of the desired point in degrees. Latitude is positive north, longitude positive east.
AMAGLT	The modified magnetic dip for the desired location. This parameter may either be calculated as described in ERL107-ITS 75 or extracted from Figure 2 of that report. AMAGLT is expressed in degrees with positive being north.
TIME	Expressed in universal hour angle from -180 to +180 degrees.
RATIO	Output parameter, $\left[\frac{f_o(F2)_i}{f_o(F2)_{SAG}}\right]^2$

Subroutine SAGMAX computes the peak daily value of $[f_o(F2)_{SAG}]^2$. This parameter is used as the denominator in the variable RATIO, output from TEC.

```
      SUBROUTINE TEC(K,U,ALAT,ALON,AMAGLT,TIME,RATIO)
      DIMENSION K(10),U(17,76),C(8),S(8),G(76),D(76),COORD(3)
      COORD(1) = AMAGLT
      COORD(2) = ALON
      COORD(3) = ALAT
      NT = K(9) + 1
      CALL GK(K,COORD,G)
      CALL SICOJT(8,C,S,TIME)
      CALL DKSICO(NT,K(10),U,S,C,D)
      CALL DKGK(NT,G,D,ANS)
      ANS = ANS*ANS
      CALL SAGMAX(K,U,SMAX)
      RATIO = ANS/SMAX
      RETURN
      END


      SUBROUTINE SAGMAX(K,U,SMAX)
      DIMENSION K(10),U(17,76),C(8),S(8),G(76),D(76),SAG(3)
      DATA SAG/55.0,-75.0,40.0/
      NT = K(9) + 1
      CALL GK(K,SAG,G)
      BIG = 0.0
      DO 10 I=1,24
      T = 15*I-180
      CALL SICOJT(8,C,S,T)
      CALL DKSICO(NT,K(10),U,S,C,D)
      CALL DKGK(NT,G,D,ANS)
      ANS = ANS*ANS
      IF(BIG.LT.ANS)  BIG = ANS
10    CONTINUE
      SMAX = BIG
      RETURN
      END


      SUBROUTINE DKSICO( MX,LH,U,S,C,D)
      DIMENSION U(17,76),C(8),S(8),D(76)
      DO 5 K=1,MX
      D(K) = U(1,K)
      DO 5 L=1,LH
 5    D(K) = D(K) + U(2*L,K)*S(L) + U(2*L+1,K)*C(L)
      RETURN
      END


      SUBROUTINE DKGK(MX,G,D,ANS)
      DIMENSION G(76),D(76)
      ANS = 0.0
      DO 5 K=1,MX
 5    ANS = ANS + D(K)*G(K)
      RETURN
      END
```

```
      SUBROUTINE  GK(K,C,G)
C
C     COMPUTE COORDINATE FUNCTIONS, G(I), I=1,....K+1
C     C(1)=MODIFIED LATITUDE. C(2), C(3), =GEOG.  LONGITUDE AND LATITUDE
      DIMENSION  K(1), C(1), G(1)
      DATA  DR/0.017453293/,N/8/
      X=DR*C
      Y=C(2)*DR
      Z=DR*C(3)
      KO=K
      SX=SIN(X)
      G(2)=SX
      G=1.
      IF (KO .EQ. 1) GO TO 12
    4 DO 10 I=2,KO
   10 G(I+1)=SX*G(I)
   12 KDIF=K(2)-KO
      IF (KDIF .NE. 0) GO TO 16
   80 RETURN
   16 J=1
      CX1=COS(Z)
      CX=CX1
      T=Y
   18 KC=K(J)+4
      G(KC-2)=CX*COS(T)
      G(KC-1)=CX*SIN(T)
   20 KN=K(J+1)
      IF (KDIF .EQ. 2) GO TO 28
      IF (KC.GT. 75) GO TO 26
      DO 22 I=KC,KN,2
      G(I)=SX*G(I-2)
   22 G(I+1)=SX*G(I-1)
   28 IF (J .EQ. N) GO TO 80
   30 KDIF=K(J+2)-KN
      IF (KDIF .EQ. 0) GO TO 80
   32 CX=CX*CX1
      J=J+1
      FJ=J
      T=FJ*Y
      GO TO 18
      END


      SUBROUTINE  SICOJT(L,C,S,A)
C
C     COMPUTE SIN(JT), COS(JT), ... ,L FOR ANGLE A
C
      DIMENSION C(1), S(1)
      T=0.01745329*A
      C=COS(T)
      S=SIN(T)
      DO 10 I=2,L
      C(I)=C*C(I-1)-S*S(I-1)
   10 S(I)=C*S(I-1)+S*C(I-1)
      RETURN
```

UNCLASSIFIED
Security Classification

DOCUMENT CONTROL DATA - R & D

(Security classification of title, body of abstract and indexing annotation must be entered when the overall report is classified)

1. ORIGINATING ACTIVITY (Corporate author)	2a. REPORT SECURITY CLASSIFICATION
Hq Air Weather Service Scott AFB, Illinois 62225	Unclassified
	2b. GROUP N/A

3. REPORT TITLE

A Model of Ionospheric Total Electron Content

4. DESCRIPTIVE NOTES (Type of report and inclusive dates)

Technical

5. AUTHOR(S) (First name, middle initial, last name)

Allan C. Ramsay, Major, USAF

6. REPORT DATE	7a. TOTAL NO. OF PAGES	7b. NO. OF REFS
June 1970	34	26

8a. CONTRACT OR GRANT NO.	9a. ORIGINATOR'S REPORT NUMBER(S)
N/A b. PROJECT NO.	Air Weather Service Technical Report 234
c.	9b. OTHER REPORT NO(S) (Any other numbers that may be assigned this report)
d.	N/A

10. DISTRIBUTION STATEMENT

This document is subject to special export controls and each transmittal to foreign governments or foreign nationals may be made only with prior approval of Hq Air Weather Service, (DN).

11. SUPPLEMENTARY NOTES	12. SPONSORING MILITARY ACTIVITY
N/A	Hq Air Weather Service Scott AFB, Illinois 62225

13. ABSTRACT

A method for specifying or predicting the total electron content of an undisturbed mid-latitude ionosphere during the maximum phase of the solar cycle is presented. The report is operationally-oriented; procedures are suitable for hand calculations and are based on readily-available information. Diurnal, seasonal, and solar-activity-related variations in total electron content are modeled.

DD FORM 1 NOV 68 1473

UNCLASSIFIED
Security Classification

14. KEY WORDS	LINK A		LINK B		LINK C	
	ROLE	WT	ROLE	WT	ROLE	WT
Ionosphere Total Electron Content Navigation Systems Range Measurement Errors						

DEPARTMENT OF THE AIR FORCE
AIR FORCE COMBAT CLIMATOLOGY CENTER (AFWA)
ASHEVILLE, NORTH CAROLINA 28801-5002

19 April 2005

MEMORANDUM FOR DTIC-OQ

ATTENTION: LARRY DOWNING
8725 JOHN J. KINGMAN ROAD
FORT BELVOIR, VA 22060-6218

FROM: Air Force Weather Technical Library
151 Patton Ave, Rm 120
Asheville, NC 28801-5002

SUBJECT: CHANGE CLASSIFICATION AND DISTRIBUTION STATEMENTS

1. AD873241 – A model of ionospheric total electron content.
2. AD117710 – Constant-pressure trajectories.
3. AD265052 – List of translations on meteorology and atmospheric physics, vol.II.
4. AD284757 – List of translations on meteorology and atmospheric physics, vol.III.
5. AD862101 – Meteorological resources and capabilities in the '70's. Proceedings of the 5th AWS Technical Exchange Conference, Air Force Academy, 14-17 July 1969.
6. AD227459 – List of translations on meteorology and atmospheric physics, vol.I.

All the above documents need to be changed to "Approved for Public Release, Distribution Unlimited" please.

Susan A. Tarbell

SUSAN A. TARBELL
Librarian, Classified Custodian,
DTIC Point of Contact

Attachment:
1. 6 copies of front covers